HHS Public Access

Author manuscript

J Invest Dermatol. Author manuscript; available in PMC 2018 November 23.

Published in final edited form as:

J Invest Dermatol. 2017 May ; 137(5): 1025–1032. doi:10.1016/j.jid.2016.11.042.

Abcc6 Knockout Rat Model Highlights the Role of Liver in PPi Homeostasis in Pseudoxanthoma Elasticum

Qiaoli Li[1,*], **Joshua Kingman**[1], **Koen van de Wetering**[1], **Sami Tannouri**[2], **John P. Sundberg**[3], and **Jouni Uitto**[1]

[1]Department of Dermatology and Cutaneous Biology, The PXE International Center of Excellence in Research and Clinical Care, The Sidney Kimmel Medical College at Thomas Jefferson University, Philadelphia, PA, USA

[2]Department of Surgery, The Sidney Kimmel Medical College at Thomas Jefferson University, Philadelphia, PA, USA

[3]The Jackson Laboratory, Bar Harbor, ME, USA

Abstract

Pseudoxanthoma elasticum (PXE), a heritable ectopic mineralization disorder, is caused by mutations in the *ABCC6* gene primarily expressed in the liver and the kidneys. The fundamental question on pathogenesis of PXE, whether lack of *ABCC6* expression in liver or kidney is the primary site of molecular pathology in peripheral tissues, has not been addressed. We generated a series of *Abcc6*$^{-/-}$ rats as models of PXE depicting ectopic mineralization in the skin, eyes, and the arterial blood vessels. Plasma PPi level was reduced (<30%) in the *Abcc6*$^{-/-}$ rats leading to lowered PPi/Pi plasma ratio. *In situ* liver and kidney perfusions were performed to determine the relative contribution of these organs to PPi levels in circulation. PPi levels in the perfusates both in the liver and kidney of *Abcc6*$^{-/-}$ rats were significantly reduced, but the PPi levels in the liver perfusates of wild type rats were 10-fold higher than that in the kidney perfusates. These observations suggest a critical role of hepatic ABCC6 in contributing to plasma PPi levels, identifying liver as a target of molecular correction to counteract ectopic mineralization in PXE.

Keywords

Pseudoxanthoma elasticum; ectopic mineralization; rat model; inorganic pyrophosphate

INTRODUCTION

Ectopic mineralization, *i.e.*, deposition of calcium and phosphate complexes in soft connective tissues, is a feature of several clinical conditions, including aging, cancer, diabetes, and autoimmune diseases (Giachelli, 1999). A number of heritable single gene

[*]Address for Correspondence: Qiaoli Li, Ph.D., Department of Dermatology and Cutaneous Biology, Sidney Kimmel Medical College at Thomas Jefferson University, 233 S. 10th Street, Suite 431 BLSB, Philadelphia, PA 19107, Qiaoli.Li@jefferson.edu.

DISCLOSURE

Dr. Sundberg has sponsored research with BIOCON which has no relevance to this project. All other authors state no conflict of interest.

disorders serve as model systems to provide insights into the pathomechanistic details of ectopic mineralization. The prototype of such conditions is pseudoxanthoma elasticum (PXE), a multisystem disorder with variable phenotypic spectrum. While ectopic mineralization affects a number of tissues in PXE, the clinical manifestations are primarily evident in the skin, eyes and the cardiovascular system (Neldner, 1988). The initial diagnosis is usually made by finding yellowish papules which coalesce to form lax and inelastic skin. The cardiovascular complications include nephrogenic hypertension, intermittent claudication, and occasionally, early myocardial infarcts and stroke. The ophthalmologic findings consist of angioid streaks reflecting mineralization of Bruch's membrane behind the pigmented retina. Breaks in the mineralized Bruch's membrane allow growth of capillaries which eventually cover the retina, leading to loss of visual acuity and blindness. PXE is characteristically a late-onset and slowly progressive disease with considerable intrafamilial and interfamilial heterogeneity.

The classic form of PXE is caused by mutations in the *ABCC6* gene (Bergen *et al.*, 2000; Le Saux *et al.*, 2000; Ringpfeil *et al.*, 2000). ABCC6 belongs to a family of ATP-binding cassette transporters which are involved in the transport of a variety of substrates across cell membranes. The physiological role of ABCC6 is currently unknown, and in particular, the factor(s) that are transported *in vivo* has not been identified. It has been demonstrated, however, that ABCC6 is involved in extracellular release of ATP, with subsequent conversion of ATP to AMP and inorganic pyrophosphate (PPi) by the ectonucleotidase ENPP1 (Jansen *et al.*, 2013; Jansen *et al.*, 2014; Li *et al.*, 2016). Since PPi is a powerful anti-mineralization factor while Pi creates a pro-mineralization environment, it has been suggested that maintaining an appropriate PPi/Pi ratio is critical for preventing aberrant mineralization under homeostatic calcium and phosphate plasma concentrations (Li *et al.*, 2016; Rosenthal and Ryan, 2016).

ABCC6 is expressed primarily in the basolateral surface of hepatocytes in the liver and in proximal tubules of the kidneys, and expression in tissues directly affected by ectopic mineralization is very low or essentially absent (Belinsky and Kruh, 1999; Scheffer *et al.*, 2002). These observations have raised two critical questions relating to the pathogenesis of PXE. First, what are the mechanisms by which mutations in the *ABCC6* gene lead to ectopic mineralization of peripheral soft connective tissues? In this regard, several early observations, including reciprocal skin grafting and parabiosis experiments in mice, suggested that PXE is a metabolic disorder reflecting the absence of a factor(s) in the circulation which under normal homeostatic conditions prevents ectopic mineralization (Jiang *et al.*, 2009; Jiang *et al.*, 2010). The second question in relation to the pathomechanisms of PXE relates to the site of molecular pathology, *i.e.*, is the absence of functional ABCC6 in the liver or in the kidneys (or both) critical for ectopic mineralization in this disorder?

Early development of *Abcc6*$^{-/-}$ mice and subsequent identification of a number of spontaneous mutant mice with sequence variations in *Abcc6* have provided model systems to examine the pathomechanisms and explore potential treatment modalities of PXE (Berndt *et al.*, 2013; Gorgels *et al.*, 2005; Klement *et al.*, 2005). However, primarily because of their small size, mice have proven difficult to explore metabolic and physiologic abnormalities

and specifically to unravel the role of Pi and PPi homeostasis in PXE. In this study, a series of *Abcc6*$^{-/-}$ rats were created using zinc finger nuclease technology. The rats, ten times larger than mice, are more suitable for investigation of the pathomechanistic details of PXE. In addition, these rats allowed us to perform *in situ* liver and kidney perfusion experiments, leading to the conclusion that liver is the primary site of molecular pathology in PXE.

RESULTS

Rat *Abcc6* is expressed in the liver and kidneys

To determine the tissue-specific expression of the rat *Abcc6* gene at the transcriptional level, various tissues from wild type Sprague Dawley rats were examined by quantitative RT-PCR on two sets of cDNA samples (Fig. S1). The first set utilized a commercial cDNA panel from eight different rat tissues. The results indicated relatively high levels of *Abcc6* mRNA in the liver, whereas low level of expression was noted in the kidney (~5% of that found in the liver). The skeletal muscle, whole brain, spleen, heart, lung, and testis had expression levels below the detection limit. The second set of cDNA consisted of aorta, skin, and eyes, tissues clinically affected by ectopic mineralization in PXE. No expression was noted with RT-PCR analysis using RNA isolated from these tissues as template. Collectively, our results indicate a relatively high level of expression of *Abcc6* in the liver and low level of expression in the kidney in rats, whereas no expression was noted in a variety of other tissues, including those affected in PXE.

Zinc finger nuclease targets the rat *Abcc6* gene for genome editing

Two pairs of zinc finger nuclease (ZFN) plasmid constructs were designed to bind and cut the genomic DNA in the first coding exon of the rat *Abcc6* gene. To ensure cleavage efficiency and specificity of ZFNs, rat C6 cells were cultured and transfected with ZFN plasmid DNA, and genomic DNA extracted after transfection and subjected to PCR amplification of the targeted region. A CEL-I mismatch endonuclease assay, which takes advantage of the non-homologous end joining process, was used to identify cleavage of heteroduplex mismatched molecules resolved by PAGE (Fig. 1a). The presence of smaller cleavage products (149 bp and 230 bp) in comparison to the parental band (379 bp) indicated that the designed ZFN was efficient in binding and cutting at the target site of the rat *Abcc6* gene.

Mutant rats were generated with targeted mutations in the *Abcc6* gene

ZFN mRNA was microinjected into embryos of Sprague Dawley rats. A total of 21 pups were generated, and among them, 4 founder rats were identified carrying distinct deletion mutations of 10 bp, 23 bp, 10 bp, and 20 bp, respectively, all surrounding the ZFN target site (Fig. 1b, Fig. S2). These deletion mutations were predicted to cause out-of-frame translation and premature stop codon. To confirm germline transmission of the mutant alleles, the founder rats were crossed individually with wild type Sprague Dawley rats. All 4 founder rats were confirmed to be germline transmission competent. One founder rat which was originally identified to carry a 20 bp deletion in its tail was chimeric, and when crossed to wild type rats, produced heterozygous offspring which were found to carry either a parental 20 bp deletion or a new 11 bp deletion. Thus, a total of five *Abcc6* mutant rat lines were

obtained harboring various sizes of deletion mutations in their *Abcc6* gene. These five mutant rats were registered at the Rat Genome Database (RGD), the premier repository for genetic, genomic, phenotype, and disease data generated from rat research. The corresponding RGD designations are SD-*Abcc6*^{em1Qlju}, SD-*Abcc6*^{em2Qlju}, SD-*Abcc6*^{em3Qlju}, SD-*Abcc6*^{em4Qlju}, and SD-*Abcc6*^{em5Qlju} (International Rat Genetic Nomenclature, 2015), with deletions of 10 bp, 23 bp, 10 bp, 20 bp, and 11 bp in the *Abcc6* gene, respectively (Fig. 1b, Fig. S2). These rat lines are designated in this study as Lines 1–5.

Three of the mutant lines, Lines 2, 3 and 4, were further bred to establish stable colonies of *Abcc6* wild type as well as their respective heterozygous and homozygous mutant animals. The distribution of the mutant genotype and the gender were subsequently determined in pups from heterozygous matings. The distribution of the genotype for the wild type, heterozygous, and homozygous mutant rats did not statistically differ from the expected 1:2:1 ratio (Chi-squared test; $P > 0.01$), and the male/female ratio was approximately 1:1, all consistent with autosomal recessive inheritance without sex preference (Table S1). All rats were maintained on standard rodent diet for further phenotypic, metabolic and physiologic analysis.

To confirm that these *Abcc6* mutant rats were negative for ABCC6 expression, the liver from the wild type and mutant rats (Line 2) was subjected to double immunofluorescent labeling with antibodies recognizing ABCC6 and Na,K-ATPase, the latter being a plasma membrane marker at the basolateral side of hepatocytes (Wolters *et al.*, 1991). The results demonstrate that, like in human and mouse, rat ABCC6 is expressed in the basolateral plasma membrane of hepatocytes in wild type rats in the plasma membrane (Fig. 1c). In contrast, immunofluorescent labeling for ABCC6 in the *Abcc6* mutant rats was entirely negative (Fig. 1c). These rats, are therefore, true knockouts (null alleles).

Abcc6$^{-/-}$ rats develop ectopic mineralization in connective tissues and serve as a model for PXE

The rats, representing three mutant lines, Lines 2, 3, and 4, were subjected to complete necropsy to examine tissue mineralization in a systematic manner, as described previously (Berndt *et al.*, 2013; Li *et al.*, 2013; Li *et al.*, 2014a; Li *et al.*, 2014b). Histopathological examination of homozygous rats from the three mutant lines on standard rodent diet demonstrated extensive mineralization in the dermal sheath of vibrissae as well as in a number of internal organs when examined by hematoxylin and eosin (H&E) or Alizarin red stains (Fig. 2a). Specifically, the dermal sheath of vibrissae in muzzle skin and the dermal sheath of mustaceal and periorbital vibrissae in eyelids were noted to be mineralized as early as at 8–12 weeks of age. In addition, mineralization was noted in the aorta, arterial blood vessels, as well as in the ventral and dorsal skin, and in the retina (Fig. 2a). No mineralization was noted in these tissues in the heterozygote and wild type rats. There were focal areas of mineralization in the kidneys of the wild type and heterozygous rats kept on standard diet, and markedly increased mineralization was noted in homozygous rats, as determined by histopathology (Fig. 2a). Spontaneous nephrocalcinosis is common in laboratory rats (Gray *et al.*, 1982), and focal mineralization of renal tubules at the cortico-

medullary junction is a frequent finding. The Sprague Dawley strain is one of the most susceptible strains to chronic progressive nephrosis, especially in female rats with spontaneously occurring tubular mineralization at the cortico-medullary junction (Solleveld and Boorman, 1986).

The mineralization of the dermal sheath of vibrissae and eyelids in mutant Line 2 was monitored non-invasively by semi-quantitative micro-computed tomography (microCT). At 2 months of age, the *Abcc6*$^{-/-}$ rats on standard diet did not show evidence of mineralization, while at 3 months of age there was clearly detectable mineralization in the muzzle skin and eyelids which progressed up to 6 months of age, a finding that was not present in the wild type rats (Fig. 2b). *Abcc6*$^{-/-}$ rats from the mutant Line 2 were also placed at weaning (~4 weeks of age) on an “acceleration diet” (enriched in phosphate and low in magnesium which promotes early onset and severity of PXE lesions in mice) for further analysis of tissue mineralization (Jiang and Uitto, 2012). Significantly increased amounts of mineral deposits were noted in *Abcc6*$^{-/-}$ rats when maintained on the acceleration diet (Fig. 2b).

The composition of mineral deposits was analyzed by energy dispersive X-ray of the mineralized areas in the vibrissae of mutant Line 2 (Kavukcuoglu *et al.*, 2012). The analysis revealed calcium and phosphorus as the principal ions in atomic ratio of 1.57 ± 0.05 (mean ± S.E.), similar to hydroxyapatite in mature endochondral bone of 1.67 (Fig. S3a). Topographic mapping revealed that these ions co-localize in the mineralized connective tissue capsule, suggesting the presence of hydroxyapatite (Fig. S3b-d).

The extent of mineralization was quantitated by a chemical assay for calcium in the biopsies of muzzle skin containing the vibrissae in rats at 12 weeks of age in mutant Line 2. The results showed a marked, up to 3.3-fold, increase in mineral content in homozygous rats compared with wild type littermates on standard diet (Fig. 2c). Heterozygotes were indistinguishable from wild type rats with respect to phenotype, histopathology, and the calcium content of the muzzle skin. When the homozygous rats were maintained on “acceleration diet”, the chemical calcium assay demonstrated significantly more mineral content in the muzzle skin than homozygous rats kept on standard diet.

Abcc6$^{-/-}$ rats have reduced plasma PPi/Pi ratio, promoting ectopic mineralization

To further examine the consequences of ABCC6 deficiency, mutant Line 2 was further analyzed by determining the concentrations of PPi in plasma of wild type, heterozygous, and homozygous mutant rats when kept on standard rodent diet. Since platelets release large amounts of PPi upon activation, which might obscure detection of differences between these rats, the PPi levels were determined in platelet-free plasma (Tolouian *et al.*, 2012). The results revealed that homozygous rats had markedly reduced PPi levels, <30% from the wild type controls, with concomitant increase in the Pi/PPi ratio, and the heterozygous mice showed intermediate levels (Table 1). These differences were not sex-dependent. The serum calcium and phosphorus levels and the corresponding Ca/P ratios were not statistically different between these three groups of rats (Table 1).

Liver and kidney perfusion studies demonstrated the critical role of liver in PPi homeostasis in PXE

ABCC6 is predominantly expressed in the liver and at low levels in the kidney. To assess whether ABCC6 is an important factor in regulating PPi/Pi homeostasis *in vivo*, we performed liver and kidney perfusion experiments followed by quantification of PPi in the perfusates. Wild type and homozygous rats generated from mutant Line 2 kept on standard diet were subjected to *in situ* perfusions of liver or kidneys. Histopathological analysis of liver and kidneys at the end of perfusion revealed no changes in morphology, integrity, or necrosis (not shown). PPi levels were clearly detected in the liver and kidney perfusates from wild type rats, while PPi levels were extremely low in perfusates collected from homozygous rats devoid of ABCC6 expression (Fig. 3). Thus the PPi levels in the liver and kidney perfusates strongly depend on the presence of ABCC6, indicating the critical role of ABCC6 expression in these tissues in providing PPi to circulation. In addition, PPi levels in kidney perfusates in wild type rats were only ~10% of the PPi levels in liver perfusates (Fig. 3). These results indicate the critical role of liver in PPi homeostasis in the pathogenesis of PXE.

DISCUSSION

Pseudoxanthoma elasticum (PXE), a protean genodermatosis, was recognized over 100 years ago to be clinically different from xanthomas (hence pseudoxanthoma), and subsequent histopathological observations of the affected skin demonstrated an abundance of pleiomorphic elastotic structures with propensity for calcification (Neldner, 1988). Demonstration of mutations a century later in the *ABCC6* gene, a putative efflux transporter of the ABC family of transmembrane proteins, when combined with clinical observations of late-onset and slow progression of disease, suggested that PXE is a metabolic disorder at the genome/environment interface (Uitto *et al.*, 2001). However, the pathomechanistic details leading from mutations in *ABCC6* to ectopic soft tissue mineralization in the peripheral tissues posed a dilemma, particularly since the naturally occurring molecules physiologically transported by *ABCC6* from the intracellular milieu to extracellular space remained unknown.

Previous observations both on human and mouse tissues indicated that ABCC6 is expressed primarily in the liver and the kidneys, and at very low levels, if at all, in tissues demonstrating ectopic mineralization in this complex disorder (Belinsky and Kruh, 1999; Scheffer *et al.*, 2002). This then raised the question whether absence of ABCC6 from the liver or the kidneys is the primary molecular defect resulting in ectopic mineralization. Efforts to answer this question using existing mouse models have been stymied primarily due to the small size of the mouse organs. In this study, a series of *Abcc6*$^{-/-}$ rats were created with time course of progression of ectopic mineralization similar to that *Abcc6*$^{-/-}$ mouse. In addition, the larger size of rats allowed us to determine plasma PPi levels and perform *in situ* perfusions and thereby assess the contribution of the liver and kidney to ABCC6-mediated extracellular PPi production.

It should be noted that while the plasma levels of PPi in the *Abcc6*$^{-/-}$ rats were low, the PPi was not completely absent, and in fact, there was ~30% of residual level measured. This may

reflect the fact that conversion of ATP to AMP and PPi by ENPP1 is not the only source of pyrophosphate in plasma. In fact, ANKH can transport PPi from chondrocytes to the extracellular milieu (Ho *et al.*, 2000). There are also a number of transport systems independent of *ABCC6* that are capable of transferring ATP from intracellular milieu to the extracellular space where it would be readily amenable for cleavage by ENPP1 (Dahl, 2015; Lohman *et al.*, 2012).

Assay of PPi concentration in the efflux perfusate in wild type rats revealed ~10-fold higher levels of PPi in the liver perfusates as compared to kidney perfusates. This observation paralleled the measurements of *Abcc6* mRNA levels in the liver and the kidneys in wild type rats, the mRNA abundance being ~17-fold higher in the liver (Fig. S1). This may reflect the fact that the most abundant cell type in the liver is hepatocyte which contains *ABCC6*. In the kidneys, ABCC6 is expressed only in the cells of proximal tubules, which make out only a minor fraction of the total population of cells in the kidney. Perfusion of $Abcc6^{-/-}$ rat liver and kidneys demonstrated very low level of PPi in the efflux perfusate, indicating that *ABCC6* is critical for generation of PPi in these two organs. Considering the quantitative differences in the release of PPi from wild type rat liver and kidneys, it is clear that liver is the major contributor of PPi to the circulation. The significance of these findings is two-fold. First, the decreased PPi/Pi ratio provides a biomarker in the mineralization process of PXE, and provides significant insight into the poorly understood link between *ABCC6* mutations and ectopic mineralization in PXE. Second, our results point to the critical role of ABCC6 in the liver in providing circulation with PPi. These findings have implications to develop organ-targeted therapeutic interventions to counteract the mineralization phenotype in PXE (Li *et al.*, 2016).

MATERIALS AND METHODS

Abcc6 gene targeting and genotyping

Zinc Finger Nuclease (ZFN) plasmid constructs were designed by Sigma-Aldrich (St. Louis, MO, USA). In brief, ZFNs were designed to target exon 1 of rat *Abcc6* gene at the binding site/cutting site 5’-CACGCCTGGAGAGTCCTGcgcaggCCTGAGGGTGAGTCC-3’ (c.24-c.62). ZFNs were transfected into rat C6 cells and tested for their efficiency in editing *Abcc6* gene using a CEL-I Assay, according to the manufacturer’s protocol (Transgenomic, Omaha, NE, USA). ZFN mRNA was microinjected into embryos from Sprague Dawley strain performed through Transgenic Animal Modeling Core Microinjection Services at University of Massachusetts Medical School. Genomic DNA from founder rats was analyzed by PCR to confirm the presence of the ZFN-induced mutation, with forward primer 5’-GGAAGTGTCTTTTCGGGGAT-3’ and reverse primer 5’-AGGACCTTGATCTGTCGCTG-3’. The amplified products were subjected to Sanger sequencing. F1 founder rats with confirmed ZFN-mediated mutations were backcrossed to wild type Sprague Dawley rats (Charles River, Wilmington, MA, USA) to ensure germline transmission. Three of the mutant lines were further bred to establish stable colonies of *Abcc6* wild type as well as their respective heterozygous and homozygous animals.

Maintenance of rats and diet

The wild type, heterozygous, and homozygous rats were generated from heterozygous matings. The rats were maintained on standard rodent laboratory diet (Laboratory Autoclavable Rodent Diet 5010; PMI Nutritional International, Brentwood, MO, USA), or on an "acceleration diet" (Harlan Teklad, Rodent diet TD.00442, Madison, WI, USA), under standard conditions (Jiang and Uitto, 2012). All protocols were approved by the Institutional Animal Care and Use Committee of Thomas Jefferson University.

Quantitative PCR

Total RNA from rat skin, eyes and aorta was isolated with Trizol reagent (Invitrogen, Carlsbad, CA, USA) followed by an RNeasy Mini Kit (Qiagen, Valencia, CA, USA). Total RNA was treated with DNase I on minicolumns to eliminate genomic DNA contamination. cDNA was synthesized from 1 μg of total RNA using the SuperScript III First-strand Synthesis kit (Invitrogen) and random hexamers. A rat cDNA panel consisting of cDNA samples from 8 rat tissues (liver, kidney, heart, whole brain, spleen, lung, skeletal muscle, and testis) was purchased (Clontech, Mountain View, CA, USA) for quantitative RT-PCR analysis. qPCR was performed using an ABI Prism 7000 sequence detection system (Applied Biosystems, Foster City, CA, USA) with Power SYBR Green PCR Master Mix. The amount of *Abcc6* mRNA per sample was quantified and normalized to *ACTB* mRNA.

Immunofluorescent labeling of ABCC6 protein on liver sections

Rat liver was quickly harvested, placed in Optimal Cutting Temperature compound and stored at −80°C. Immunofluorescent staining of liver samples was performed on 6 μm frozen sections. The rabbit polyclonal anti-rat ABCC6 antibody (K14, gift from Dr. Bruno Stieger, University Hospital, Zurich, Switzerland) was used to identify the rat ABCC6 protein. A mouse monoclonal antibody was used to label the basolateral plasma membrane marker Na,K-ATPase on the same section (Abcam, Cambridge, MA, USA). The Alexa Fluor 488 donkey anti-goat and Alexa Fluor 594 goat anti-mouse secondary antibodies (Invitrogen) were used for incubation with tissue sections for ABCC6 and Na,K-ATPase, respectively. Images were acquired with an EVOS® FL Auto Imaging Microscopy (Thermo Fisher Scientific) and Zeiss LSM Image software.

Small animal computed tomography (microCT) scan

Abcc6 wild type and homozygous rats were examined for mineralization at 2–6 months of age by small animal microCT scan. Briefly, rats were anesthetized with isofluorane and then scanned with a Siemens Inveon MicroCT Scanner (Knoxville, TN, USA). A 3-dimensional rendering was created for each rat using Amira software, version 5.3.3 (Visualization Sciences Group, Bordeaux, France, and the Zuse Institute, Berlin, Germany).

Complete necropsy and histopathological analysis

After euthanizing the rats by CO_2 asphyxiation, complete necropsies were performed (Silva and Sundberg, 2012). Tissues were collected and fixed in 10% phosphate-buffered formalin overnight then transferred and stored in 70% ethanol. Tissues were then trimmed and embedded in paraffin, cut into 6 μm sections, and stained with Hematoxylin-Eosin (H&E)

and/or Alizarin red (AR). All histology slides were reviewed by an experienced, board-certified veterinary pathologist (JPS).

Chemical quantitation of calcium and phosphate

To quantify the mineral deposition, muzzle skin biopsies were harvested and calcium was solubilized with 0.15 mol/L HCl for 48 hours at room temperature. The solubilized calcium content was determined by a colorimetric assay using the o-cresolphthalein complexone method (calcium (CPC) LiquiColor; Stanbio Laboratory, Boerne, TX, USA). The values were normalized to tissue weight. Serum calcium concentrations were determined with the same assay, and serum phosphate level was measured by the Malachite Green Phosphate Assay Kit (Bioassay Systems, Hayward, CA, USA).

Plasma collection and inorganic pyrophosphate (PPi) assay

Whole blood was collected by cardiac puncture into heparin containing syringe, transferred into a test tube and stored on ice. After centrifugation (1,000 g for 10 min, 4°C), plasma was depleted of platelets by filtration (2,200 g for 20 min, 4°C) through a Centrisart I 300 kD mass cutoff filter (Sartorius, New York, NY, USA) and stored at −80°C until further processing. PPi in plasma was measured by an enzymatic reaction using ATP sulfurylase to convert PPi into ATP in the presence of excess adenosine 5' phosphosulfate (Sigma-Aldrich), as described previously (Jansen *et al.*, 2014).

Energy dispersive X-ray analysis

Sections of muzzle skin were analyzed using energy dispersive X-ray analysis and topographic mapping (Kavukcuoglu *et al.*, 2012). Paraffin sections were mounted onto carbon carriers, imaged, and analyzed for elemental composition with a FEI 600 Quanta FEG scanning electron microscope (FEI Company, Eindhoven, The Netherlands) fitted with an Octane Super SDD EDS detector (EDAX, Sandy, UT, USA). X-ray topographic maps of calcium and phosphorus were acquired using Spirit software version 1.07.05 (Princeton Gamma-Tech, Rocky Hill, NJ, USA).

Liver and kidney perfusions

The *in situ* liver and kidney perfusions were performed by procedures that have been described previously (El-Sheikh *et al.*, 2014; Groen *et al.*, 1995), with modifications. Krebs-bicarbonate buffer solution (containing NaCl, 120 mmol/L; $NaHCO_3$, 24 mmol/L; KCl, 4.8 mmol/L; KH_2PO_4, 1.2 mmol/L; $MgSO_4$, 1.2 mmol/L; $CaCl_2$, 1.3 mmol/L; Hepes, 10 mmol/L; D-glucose, 900.8 mg/L, and BSA, 100 mg/L) was used as perfusate. The buffer was continuously gassed with carbogen (95% O_2/5% CO_2) using a carbogen tank. The temperature of the perfusate was maintained at 37°C. For liver perfusion, a catheter was placed into the portal vein (in) that provides blood to the liver. Another catheter was placed into the supra-hepatic inferior vena cava (out) that transports blood away from the liver. The inferior infra-hepatic vena cava was ligated to prevent loss of buffer to other parts of the body. This arrangement temporarily separates the liver's blood supply from circulating throughout the rest of the body and allows perfusion buffer to be directed to the liver only.

In the case of renal perfusion, both kidneys were simultaneously perfused. A catheter was placed into the abdominal aorta (in) that provides blood to the kidneys. Another catheter was placed into the inferior vena cava below the kidneys (out) that takes blood away from the kidneys. The inferior vena cava and abdominal aorta above kidneys were ligated to create an isolated circuit so that only kidneys were perfused. After all blood was drained from liver or kidneys, the outflow samples were collected through the catheter (out), placed immediately on ice, and stored at −80°C for PPi analysis as described above. At the end of perfusion, liver and kidneys were evaluated by histopathology to assess liver/kidney morphology, integrity, necrosis, and apoptosis.

Statistical analysis

Comparisons between different groups of mice were performed using the two-sided Kruskal-Wallis nonparametric test. Statistical significance was reached with $P < 0.05$. All statistical computations were completed using SPSS version 15.0 software (SPSS, Chicago, IL, USA).

Supplementary Material

Refer to Web version on PubMed Central for supplementary material.

ACKNOWLEDGMENTS

The authors thank Dian Wang, Jingyi Zhao, Yoorock Suh and Kathleen A. Silva for technical assistance. ABCC6 antibody was kindly provided by Dr. Bruno Stieger at the University Hospital, Zurich, Switzerland. Dr. Jamie Ford at Penn Engineering Nanoscale Characterization Facility at the University of Pennsylvania assisted in energy dispersive x-ray analysis. Drs. Mathew Thakur and Neil Mehta assisted in microCT scanning. Drs. Joseph Gosselin and Stephen N. Jones at the University of Massachusetts Medical School provided microinjection service. Carol Kelly helped in manuscript preparation. Dr. Li is recipient of a NIH/NIAMS Career Development Award (K01AR064766). These studies were supported by NIH/NIAMS grants R01AR028450 (JU) and R01AR055225 (JU and JPS).

Abbreviations:

PXE	pseudoxanthoma elasticum
GACI	generalized arterial calcification of infancy
ZFN	zinc finger nuclease
PPi	inorganic pyrophosphate
Pi	inorganic phosphate

REFERENCES

Belinsky MG, Kruh GD. MOAT-E (ARA) is a full-length MRP/cMOAT subfamily transporter expressed in kidney and liver. Br J Cancer 1999;80:1342–9. [PubMed: 10424734]

Bergen AA, Plomp AS, Schuurman EJ, Terry S, Breuning M, Dauwerse H, et al. Mutations in ABCC6 cause pseudoxanthoma elasticum. Nat Genet 2000;25:228–31. [PubMed: 10835643]

Berndt A, Li Q, Potter CS, Liang Y, Silva KA, Kennedy V, et al. A single-nucleotide polymorphism in the Abcc6 gene associates with connective tissue mineralization in mice similar to targeted models for pseudoxanthoma elasticum. J Invest Dermatol 2013;133:833–6. [PubMed: 23014343]

Dahl G ATP release through pannexon channels. Philos Trans R Soc Lond B Biol Sci 2015;370.

El-Sheikh AA, Koenderink JB, Wouterse AC, van den Broek PH, Verweij VG, Masereeuw R, et al. Renal glucuronidation and multidrug resistance protein 2-/ multidrug resistance protein 4-mediated efflux of mycophenolic acid: interaction with cyclosporine and tacrolimus. Transl Res 2014;164:46–56. [PubMed: 24486136]

Giachelli CM. Ectopic calcification: gathering hard facts about soft tissue mineralization. Am J Pathol 1999;154:671–5. [PubMed: 10079244]

Gorgels TG, Hu X, Scheffer GL, van der Wal AC, Toonstra J, de Jong PT, et al. Disruption of *Abcc6* in the mouse: novel insight in the pathogenesis of pseudoxanthoma elasticum. Hum Mol Genet 2005;14:1763–73. [PubMed: 15888484]

Gray JE, van Zwieten MJ, Hollander CF. Early light microscopic changes in chronic progressive nephrosis in several strains of aging laboratory rats. J Gerontol 1982;37:142–50. [PubMed: 7056999]

Groen AK, Van Wijland MJ, Frederiks WM, Smit JJ, Schinkel AH, Oude Elferink RP. Regulation of protein secretion into bile: studies in mice with a disrupted mdr2 p-glycoprotein gene. Gastroenterology 1995;109:1997–2006. [PubMed: 7498666]

Ho AM, Johnson MD, Kingsley DM. Role of the mouse ank gene in control of tissue calcification and arthritis. Science 2000;289:265–70. [PubMed: 10894769]

Jansen RS, Kucukosmanoglu A, de Haas M, Sapthu S, Otero JA, Hegman IE, et al. ABCC6 prevents ectopic mineralization seen in pseudoxanthoma elasticum by inducing cellular nucleotide release. Proc Nat Acad Sci USA 2013;110:20206–11. [PubMed: 24277820]

Jansen RS, Duijst S, Mahakena S, Sommer D, Szeri F, Varadi A, et al. ABCC6-mediated ATP secretion by the liver is the main source of the mineralization inhibitor inorganic pyrophosphate in the systemic circulation-brief report. Arterioscler Thromb Vasc Biol 2014;34:1985–9. [PubMed: 24969777]

Jiang Q, Endo M, Dibra F, Wang K, Uitto J. Pseudoxanthoma elasticum is a metabolic disease. J Invest Dermatol 2009;129:348–54. [PubMed: 18685618]

Jiang Q, Oldenburg R, Otsuru S, Grand-Pierre AE, Horwitz EM, Uitto J. Parabiotic heterogenetic pairing of Abcc6−/−/Rag1−/− mice and their wild-type counterparts halts ectopic mineralization in a murine model of pseudoxanthoma elasticum. Am J Pathol 2010;176:1855–62. [PubMed: 20185580]

Jiang Q, Uitto J. Restricting dietary magnesium accelerates ectopic connective tissue mineralization in a mouse model of pseudoxanthoma elasticum (Abcc6−/−). Exp Dermatol 2012;21:694–9. [PubMed: 22897576]

Kavukcuoglu NB, Li Q, Pleshko N, Uitto J. Connective tissue mineralization in Abcc6(−/−) mice, a model for pseudoxanthoma elasticum. Matrix Biol 2012;31:246–52. [PubMed: 22421595]

Klement JF, Matsuzaki Y, Jiang QJ, Terlizzi J, Choi HY, Fujimoto N, et al. Targeted ablation of the *Abcc6* gene results in ectopic mineralization of connective tissues. Mol Cell Biol 2005;25:8299–310. [PubMed: 16135817]

Le Saux O, Urban Z, Tschuch C, Csiszar K, Bacchelli B, Quaglino D, et al. Mutations in a gene encoding an ABC transporter cause pseudoxanthoma elasticum. Nat Genet 2000;25:223–7. [PubMed: 10835642]

Li Q, Guo H, Chou DW, Berndt A, Sundberg JP, Uitto J. Mutant Enpp1asj mouse as a model for generalized arterial calcification of infancy. Dis Model Mech 2013;6:1227–35. [PubMed: 23798568]

Li Q, Pratt CH, Dionne LA, Fairfield H, Karst SY, Sundberg JP, et al. Spontaneous *asj-2J* mutant mouse as a model for generalized arterial calcification of infancy: A large deletion/insertion mutation in the *Enpp1* gene. PLOS One 2014a;9:e113542. [PubMed: 25479107]

Li Q, Price TP, Sundberg JP, Uitto J. Juxta-articular joint-capsule mineralization in CD73 deficient mice: Similarities to patients with *NT5E* mutations. Cell Cycle 2014b;13:2609–15. [PubMed: 25486201]

Li Q, Aranyi T, Varadi A, Terry SF, Uitto J. Research progress in pseudoxanthoma elasticum and related ectopic mineralization disorders. J Invest Dermatol 2016;136:550–6. [PubMed: 26902123]

Lohman AW, Billaud M, Isakson BE. Mechanisms of ATP release and signalling in the blood vessel wall. Cardiovasc Res 2012;95:269–80. [PubMed: 22678409]

Neldner KH. Pseudoxanthoma elasticum. Clin Dermatol 1988;6:1–159.

Ringpfeil F, Lebwohl MG, Christiano AM, Uitto J. Pseudoxanthoma elasticum: mutations in the MRP6 gene encoding a transmembrane ATP-binding cassette (ABC) transporter. Proc Natl Acad Sci U S A 2000;97:6001–6. [PubMed: 10811882]

Rosenthal AK, Ryan LM. Calcium pyrophosphate deposition disease. N Engl J Med 2016;374:2575–84. [PubMed: 27355536]

Scheffer GL, Hu X, Pijnenborg AC, Wijnholds J, Bergen AA, Scheper RJ. MRP6 (ABCC6) detection in normal human tissues and tumors. Lab Invest 2002;82:515–8. [PubMed: 11950908]

Silva KA, Sundberg JP (2012) Necropsy methods In: The Laboratory Mouse (Hedrich HJ, ed) 2nd ed., London: Academic Press, 779–806.

Solleveld HA, Boorman GA. Spontaneous renal lesions in five rat strains. Toxicol Pathol 1986;14:168–74. [PubMed: 3764314]

Tolouian R, Connery SM, O'Neill WC, Gupta A. Using a filtration technique to isolate platelet free plasma for assaying pyrophosphate. Clin Lab 2012;58:1129–34. [PubMed: 23289181]

Uitto J, Pulkkinen L, Ringpfeil F. Molecular genetics of pseudoxanthoma elasticum: a metabolic disorder at the environment-genome interface? Trends Mol Med 2001;7:13–7. [PubMed: 11427982]

Wolters H, Spiering M, Gerding A, Slooff MJ, Kuipers F, Hardonk MJ, et al. Isolation and characterization of canalicular and basolateral plasma membrane fractions from human liver. Biochim Biophys Acta 1991;1069:61–9. [PubMed: 1932051]

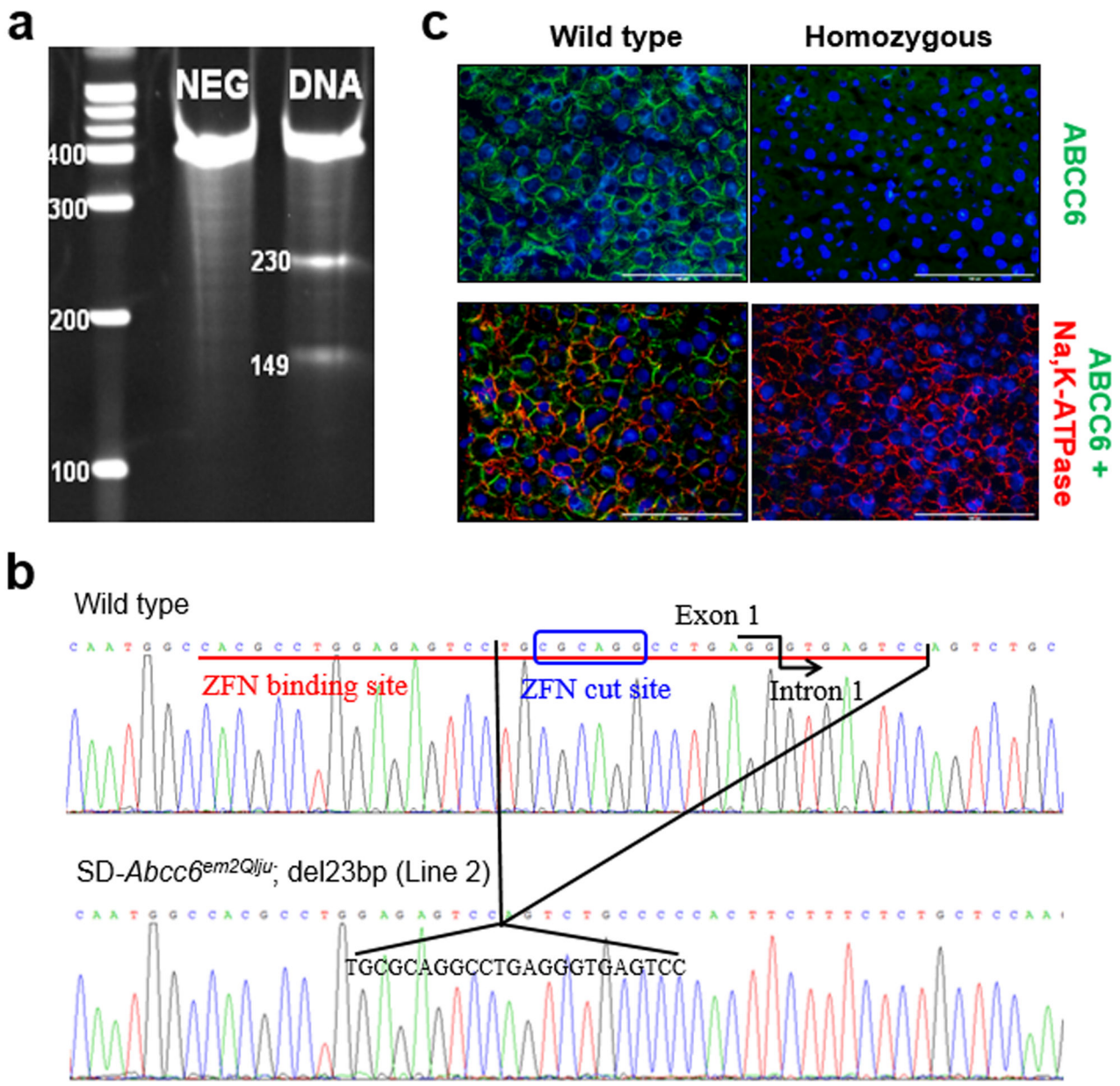

Figure 1. Generation and characterization of mutant *Abcc6*$^{-/-}$ rats.

(**a**) Surveyor Mutation Detection Assay demonstrates successfully targeted *Abcc6* gene editing. Rat C6 cell line was cultured and transfected with ZFN plasmid DNA. Total genomic DNA was extracted from transfected cells (DNA) and from control cells as a negative control (NEG) and subjected to PCR amplification. A CEL-1 digestion assay was performed on the PCR products and resolved on 10% TBE-PAGE. (**b**) Sequence comparison surrounding the ZFN target site reveals a deletion mutation of 23 bp in mutant line SD-*Abcc6*^{em2Qlju} (Line 2). The ZFN binding site is underlined, and the ZFN cut site is boxed. **(c)** The rat ABCC6 K14 antibody labeling in the wild type liver revealed the plasma membrane localization for ABCC6 (green) **(1)**, which showed significant overlap with large areas of co-localization (yellow) with the basolateral plasma membrane marker Na,K-

ATPase (red) **(2)**. Complete absence of labeling of the plasma membrane for ABCC6 protein was found in the liver of *Abcc6*$^{-/-}$ rats **(3,4)**. Scale bar, 100 μm.

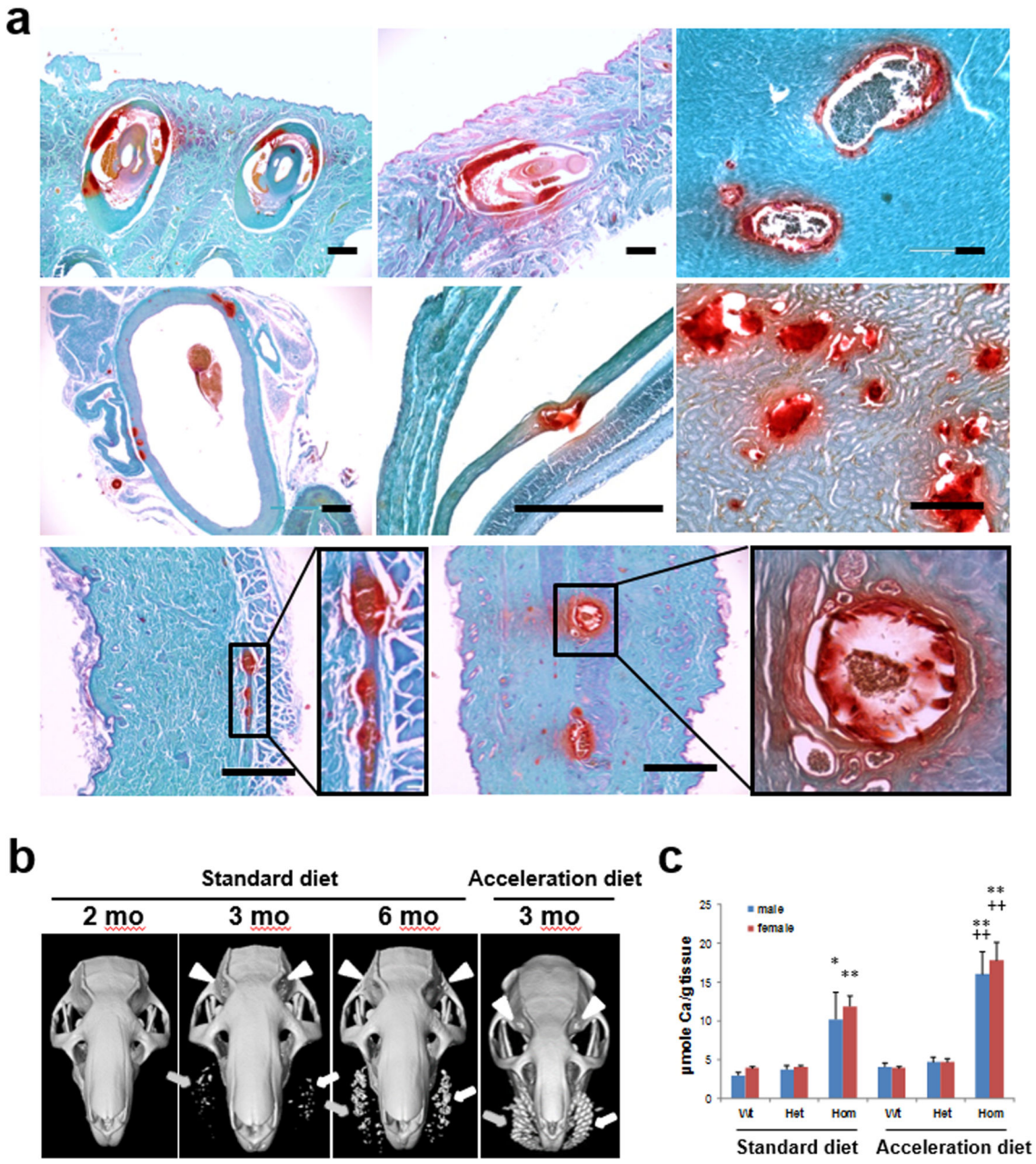

Figure 2. Characterization of ectopic mineralization in *Abcc6*$^{-/-}$ rats.

(a) Histological analysis demonstrates ectopic mineralization in a number of tissues of *Abcc6*$^{-/-}$ rats at 12 weeks of age. Alizarin red staining of tissue sections from knockout rats reveals mineralization in the dermal sheath of vibrissae in muzzle skin (top row left panel), the dermal sheath of vibrissae in the eyelids (top row middle panel), arterial blood vessels in the heart (top row right panel), aorta (middle row left panel), Bruch's membrane of the eye (middle row middle panel), kidney (middle row right panel), ventral skin (bottom row left panel), and dorsal skin (bottom row right panel). Ectopic mineralization was not noted in heterozygous or wild type rats except in the kidneys. Scale bars in the figure, 400 µm. **(b)** Computed tomography demonstrates mineralization of dermal sheath of vibrissae in

Abcc6$^{-/-}$ rats. When *Abcc6*$^{-/-}$ rats were maintained on standard rodent diet (left three panels), mineralization of dermal sheath of vibrissae in both muzzle skin (indicated by arrows) and eyelids (indicated by arrowheads) was clearly detectable at 3 months of age and progressing at 6 months of age. No mineralization was present at 2 months of age (the left panel). The *Abcc6*$^{-/-}$ rats develop significantly more mineralization when placed on "acceleration diet", as shown at 3 months of age (right panel; compare with the rat at 3 months of age on standard diet). **(c)** Quantitation of mineralization by chemical assay of calcium in muzzle skin containing the dermal sheath of vibrissae of rats at 12 weeks of age kept on either standard diet or acceleration diet. Marked increase in mineralization is noted in the vibrissae of homozygous rats in comparison with wild type or heterozygous animals. The homozygous rats mineralize more when placed on acceleration diet. The values are mean ± S.E., n = 5 – 9 rats per sex in each group. Wt, wild type; Het, heterozygous; Hom, homozygous. Statistical significance: * $P < 0.05$, ** $P < 0.01$ versus wild type rats on the same diet; $^{++}$ $P < 0.01$ versus homozygous rats on the standard diet.

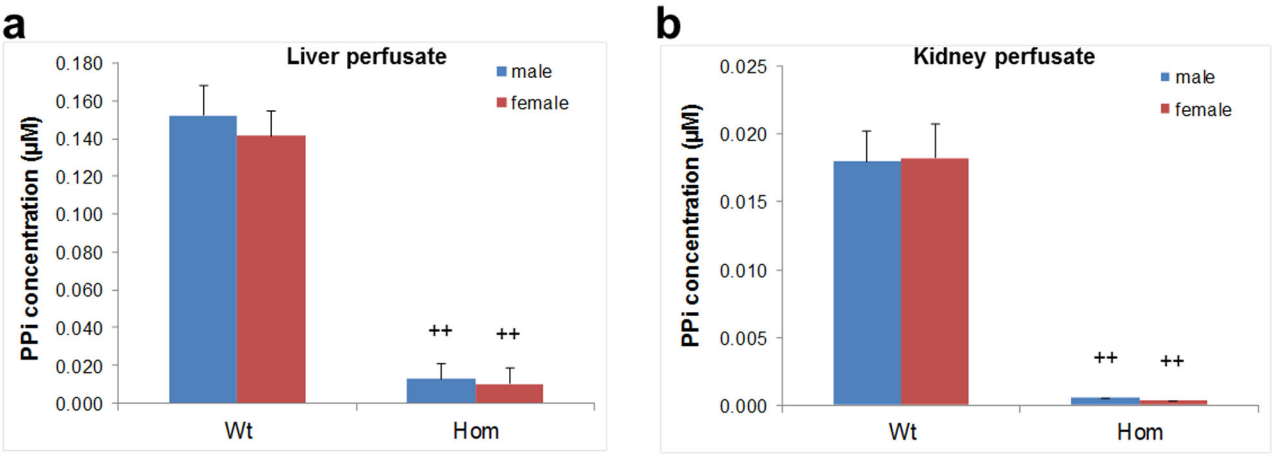

Figure 3. Quantification of PPi levels in liver and kidney perfusates of wild type and *Abcc6*$^{-/-}$ rats.

The PPi levels in the perfusates of *Abcc6*$^{-/-}$ rats were significantly lower as compared to that in the wild type rats. (**a**) liver perfusate; (**b**) kidney perfusate. Note the differences in the scale of the vertical axis demonstrating that PPi levels in the liver perfusate were ~10-fold higher than in kidney perfusate of wild type rats. Wt, wild type; Het, heterozygous; Hom, homozygous. Five males and 5 females in each group were analyzed; mean ± S.E.; $^{++}$, $P <$ 0.001.

Table 1.

Blood parameters in *Abcc6* wild type, heterozygous, and homozygous rats in SD-*Abcc6*^{em2Qlju} mutant line (Line 2)*

Genotype	Sex	Serum/plasma concentration (mean ± S.E.)				
		Ca^{2+} (mg/dl)	Pi (mg/dl)	Ca/Pi ratio	PPi (μM)	Pi/PPi ratio
Wt	male	10.8 ± 0.4	7.0 ± 0.3	1.56 ± 0.06	1.08 ± 0.17	455.3 ± 54.2
Wt	female	9.7 ± 0.2	5.9 ± 0.2	1.61 ± 0.06	0.77 ± 0.11	558.9 ± 97.9
Het	male	10.0 ± 0.3	7.1 ± 0.6	1.44 ± 0.08	0.61 ± 0.08 +	820.6 ± 144.1
Het	female	10.1 ± 0.2	5.7 ± 0.1	1.76 ± 0.05	0.53 ± 0.04	710.9 ± 48.5
Hom	male	10.5 ± 0.2	7.1 ± 0.5	1.53 ± 0.120	0.29 ± 0.07 ++	2082.3 ± 626.9 +
Hom	female	10.2 ± 0.3	5.9 ± 0.2	1.73 ± 0.04	0.24 ± 0.05 ++	1925.5 ± 479.2 +

* The rats were maintained on standard rodent diet. Wt, wild type; Het, heterozygous; Hom, homozygous.

Statistical significance in comparison to sex-matched wild type rats is indicated:

+ $p < 0.05$;

++ $p < 0.01$ (Five male and 5 female rats per sex in each group). Calcium and P_i were measured in serum samples, and PP_i was measured in heparinized plasma samples.